Hindawi Publishing Corporation
International Journal of Antennas and Propagation
Volume 2012, Article ID 413683, 13 pages
doi:10.1155/2012/413683

Research Article

Indoor Off-Body Wireless Communication: Static Beamforming versus Space-Time Coding

Patrick Van Torre,[1,2] Maria Lucia Scarpello,[1] Luigi Vallozzi,[1] Hendrik Rogier,[1] Marc Moeneclaey,[3] Dries Vande Ginste,[1] and Jo Verhaevert[2]

[1] *Department of Information Technology (INTEC), Ghent University, St. Pietersnieuwstraat 41, 9000 Ghent, Belgium*
[2] *Faculty of Applied Engineering Sciences (INWE), University College Ghent, Valentin Vaerwyckweg 1, 9000 Gent, Belgium*
[3] *Department of Telecommunications and Information Processing (TELIN), Ghent University, St. Pietersnieuwstraat 41, 9000 Ghent, Belgium*

Correspondence should be addressed to Patrick Van Torre, patrick.vantorre@ugent.be

Received 25 July 2011; Revised 20 October 2011; Accepted 22 October 2011

Academic Editor: Yan Zhang

The performance of beamforming versus space-time coding using a body-worn textile antenna array is experimentally evaluated for an indoor environment, where a walking rescue worker transmits data in the 2.45 GHz ISM band, relying on a vertical textile four-antenna array integrated into his garment. The two transmission scenarios considered are static beamforming at low-elevation angles and space-time code based transmit diversity. Signals are received by a base station equipped with a horizontal array of four dipole antennas providing spatial receive diversity through maximum-ratio combining. Signal-to-noise ratios, bit error rate characteristics, and signal correlation properties are assessed for both off-body transmission scenarios. Without receiver diversity, the performance of space-time coding is generally better. In case of fourth-order receiver diversity, beamforming is superior in line-of-sight conditions. For non-line-of-sight propagation, the space-time codes perform better as soon as bit error rates are low enough for a reliable data link.

1. Introduction

Reliable wireless data communication is of paramount importance for rescue workers operating in indoor environments. Smart garments for professionals active during emergency situations contain integrated sensors and a transmitting system for sending the collected data to the command center in real time [1].

The indoor environment where interventions are performed exhibits line-of-sight (LoS) as well as non line-of-sight (NLoS) radio propagation conditions. The received signals experience Ricean or Rayleigh fading, often with additional lognormal shadowing, easily producing variations in signal-to-noise ratio (SNR) exceeding 35 dB [2, 3].

1.1. Motivation. Experimental data comparing the performance of beamforming and space-time coding (STC) transmissions are scarce in literature. In case of off-body communication links, a literature search revealed no experimental results. Theoretically, for LoS conditions, the received signals can be significantly enhanced by using beamforming techniques. However, for off-body communication in an indoor environment, beamforming is not straightforward, especially when relying on flexible textile antennas directly deployed on the human body. In addition to significant multipath effects and shadowing by the human body, many factors influence array performance, such as the proximity of the human body to the wearable antenna elements and movements of the body as well as deformation of the flexible textile array affecting the orientation of the beam. Shadowing by the body can cause blocking of the direct path in the LoS environment, but a large beam width in the azimuth plane will significantly increase the portion of signals received via dominant specular reflections at walls and office equipment.

By performing beamforming using a vertical array, the transmitted power is concentrated in the elevation direction along the direct path between the transmitter and the receiver, resulting in an increased average received signal level and reducing the number of paths contributing to fading. However, the interference between direct and reflected signals can still cause significant fading, which is detrimental to the bit error rate (BER) performance. Additional receiver diversity using maximum-ratio combining (MRC) can mitigate these fading effects. Previous measurements in our indoor environment, documented in [4], confirmed substantial diversity gain for fourth-order receive diversity with two dual-polarized antennas. Beamforming is preferred in the elevation direction only, to accommodate for movements of the rescue worker. For a walking person, the rotation of the array in the elevation plane is minimal, allowing static low-elevation angle beamforming. Beamforming in the azimuth plane is not advised as the actual orientation of the rescue worker in the azimuth plane is assumed to be unpredictable. For NLoS propagation, the rich scattering of the signals in the environment includes waves propagating at higher elevation angles. Therefore, it is interesting to transmit with a wide-elevation coverage. Thanks to their high beamwidth and higher diversity order, transmit diversity techniques such as space-time codes are expected to outperform static beamforming systems [5] for NLoS propagation conditions.

Adaptive beamforming could in principle further enhance the communication as compared to static beamforming but requires continuous feedback of channel information from the receiver to the transmitter [6]. For a rescue worker operating in an indoor environment, the channel response often varies significantly within a fraction of a second [2], therefore, high-rate channel information feedback would be necessary, introducing a large overhead in the communication and requiring more complex hardware.

In terms of implementation complexity and energy consumption, static beamforming is preferred over STC. Static beamforming can be realized by simply using phase shifters, whereas STC requires complex and more power-consuming hardware with dedicated transmit chains for each channel. Additional diversity reception is an important option to further improve the error performance, increasing complexity at the base station but not at the transmitter.

1.2. Previous Work. A very limited set of measurements comparing beamforming to STC is available in literature and the available material covers no body-centric applications, hence, they are not dealing with direct shadowing by the human body. An experimental comparison of MIMO and beamforming schemes is presented in [7, 8]. These papers focus on channel capacity, and the measurements are for an outdoor-to-indoor scenario, with a fixed transmitter and the receiver in a number of fixed positions. Horizontal antenna arrays are used at both the transmitter and receiver. The related propagation conditions are different from those for a walking person with a body-worn vertical antenna array.

The literature study revealed many simulations and analytical results. Space-time codes were studied in combination with beamforming at the receiver for interference rejection in [9]. Alternatively, depending on propagation conditions, a number of transmit beams can be formed, in combination with an appropriately sized space-time code [10–12]. Often the proposed schemes use environment-oriented adaptive beamforming, forming a directive beam pattern toward the impinging waves' directions-of-arrival. This is more appropriate for situations where the angles-of-arrival of the signals are fairly constant [10, 13, 14]. Others propose optimal power allocation for beamforming based on statistical channel information [15–17] or imperfect instantaneous channel state information [18, 19].

A numerical comparison between beamforming and space-time coding is documented in [20, 21], confirming the better performance of space-time codes in NLoS conditions with large feedback delay, because of the higher diversity gain. In [18], the performance of both techniques is compared as a function of the quality of the channel feedback information. In [22], an interesting scheme is proposed with a performance converging to conventional space-time coding with low-rate and erroneous channel estimation feedback and to directional beamforming with high-rate and error-free channel estimation feedback.

However, for wearable applications, systems with low weight, low cost, and low power consumption are desired. The need for a feedback channel often makes the proposed scheme not compatible with these requirements. Note that an off-body system is likely to require a high-rate feedback channel due to the quickly changing channel response for a walking person in an indoor fading environment.

1.3. Own Contributions. In contrast to scenarios in existing literature, the transmit array is flexible and directly deployed on the body of a moving user. Only static beamforming is considered because of the rapidly changing channel conditions experienced by a walking person. The aim of this paper is to experimentally investigate the performance gain realized by confining a transmit beam along zero elevation (for communication with a receiver located on the same floor of the building) by means of a vertically oriented textile antenna array integrated into a firefighter suit, and to compare this beamforming gain with diversity gain realized by means of space-time codes relying on the same array. By creating a relatively broad beam in the azimuth plane, the wearable vertical array also provides some beamforming gain in case of dominant specular reflection, even when the direct path is blocked by the wearer's body.

In the following measurement campaign, static beamforming SISO and 1×4 SIMO systems are compared to space-time coded 4×1 MISO and 4×4 MIMO links, respectively. All measurements are performed in the 2.45 GHz ISM (industrial, scientific, and medical) band. The measurements confirm the better performance of space-time coding in NLoS conditions, similar to the numerical comparison documented in [20, 21].

Our measurements indicate that a degree of diversity is always desirable. Without receiver diversity, the space-time code performs better than beamforming for all acceptable bit error rates, due to the absence of diversity for the latter. With receiver diversity, beamforming is always better in LoS conditions, whereas for NLoS, space-time coding performs better for bit error rates lower than $3.3 \cdot 10^{-3}$.

1.4. Organization of the Paper. Section 2 documents the textile antenna array used for beamforming/transmit diversity. Section 3 discusses the transmit antenna setup, signal format, and receiver operation. Measurement results are presented in Section 4, including signal-to-noise ratios (SNRs), signal correlation coefficients, and bit error characteristics. General conclusions follow in Section 5.

2. Wearable Textile Antenna Array

At the transmit side of the off-body link, we deploy a wearable textile antenna array invisibly integrated into a firefighter suit. A uniform linear array (ULA) topology, composed of four tip-truncated equilateral triangular microstrip patch antennas (ETMPAs), was adopted. For easy low-cost beamforming, the four ETMPAs are equally spaced and fed through a 50 Ω coaxial SMA connector, manually soldered. By cutting off a triangle from one of the tips of the patch [23, 24], the size of the ETMPA can be further reduced.

The triangular patch, used as antenna element, provides radiation characteristics similar to a rectangular microstrip antenna while occupying a smaller area and guaranteeing low mutual coupling between adjacent elements. It is frequently used as a microstrip element, microstrip radiator, or for array design on rigid substrates [25], but never before on a textile substrate.

Both the patch and ground plane of the array are made of *Flectron*, a breathable and highly conductive electrotextile material, being a copper-plated nylon fabric with a surface resistivity of less than 0.10 Ω/sq.

The array is implemented on a nonconductive textile substrate, being a protective polyurethane foam called "Azzurri," manufactured by Lion [26]. Geometrical parameters of the patches and dielectric characteristics of the substrates are listed in Table 1 and indicated in Figure 1. The textile array is specifically designed for integration inside a firefighter jacket, and it is vertically positioned on the human torso, as shown in Figure 2.

The distance between patches is chosen to be $(34)\lambda$, where λ is the free-space wavelength, being approximately 122 mm, to minimize mutual coupling between two adjacent elements. The choice of 92 mm between two consecutive feeding points leads to a low-cost array implementation, as it consists of only four patches. Moreover, it is a convenient choice as the complete array, to be positioned vertically, has a large aperture, fully exploiting the size of the human torso. In fact, the design of this vertical array offers limited steering capabilities of the beam maximum in a narrow angular sector of about 10°, centered around the broadside direction, allowing to confine the energy within a narrow beam,

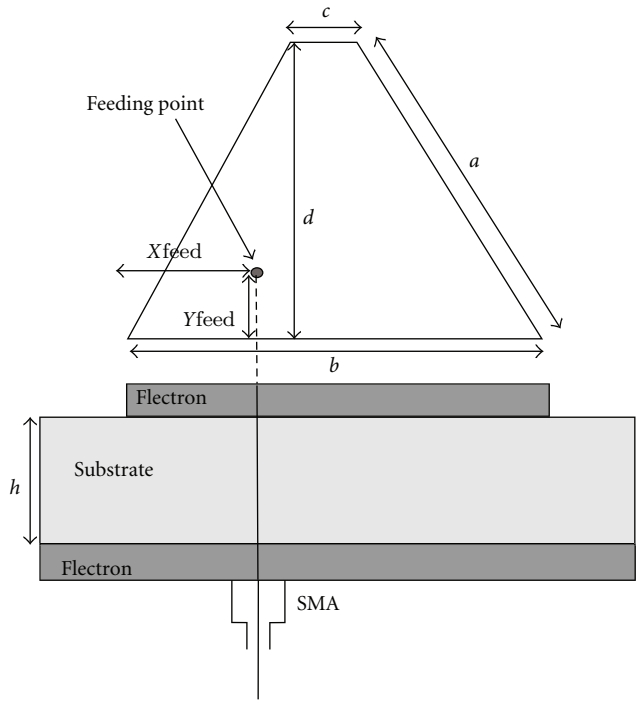

Figure 1: Side view of the textile antenna array and its geometrical dimensions.

Table 1: Tip-truncated ETMPA on the Azzurri substrate: dielectric properties and patch dimensions.

Patch (mm)		Substrate	
a	60.1	L (mm)	480
b	69	W (mm)	180
c	8.6	h (mm)	3.55
d	52.8		
Xfeed	27.5	ϵ_r	1.19
Yfeed	10	$\tan\delta$	0.003

centered around the azimuth plane. Within this steering range, it does not exhibit grating lobes. The total size of the array and the distance between two feeding points are indicated in Figure 2 and Table 1.

For the array positioned vertically, Table 2 displays the simulated and measured −3 dB beam width of a single-patch antenna and of the array at 2.45 GHz, in the elevation plane (xz-plane) and in the azimuth plane (yz-plane). It is clear that the array is quite directive in the elevation plane, compared to the single-patch element.

The beam width in the azimuth plane is always wide enough to allow for movements of the rescue worker. The beam width in the elevation plane is small, providing a higher gain along the beam maximum at zero elevation. Note that for the space-time code, the elevation beam width for a single-patch is valid.

3. Measurement Setup

3.1. Mobile Rescue Worker: Transmitted Signals. The rescue worker transmits with the vertically mounted textile antenna

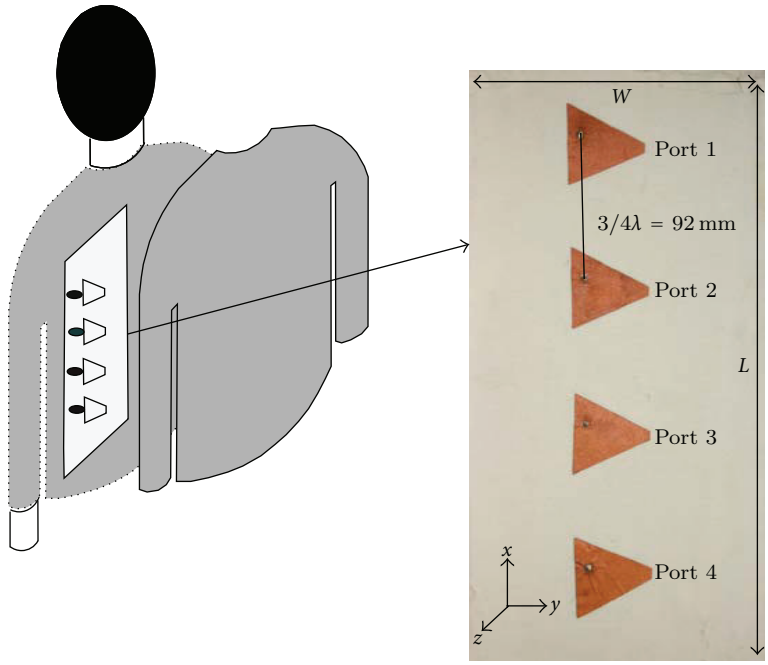

Figure 2: Top view of the textile antenna array and its position on the human body. TX1 to TX4 from top to bottom. W and L are the dimensions of the ground plane, as indicated in Table 1. The antenna array is placed on the back of the body, inside the firefighter jacket.

Table 2: Simulated and measured −3 dB beam width of a single-patch antenna and of the array, in the elevation plane (xz-plane) and in the azimuth plane (yz-plane).

	Elevation plane (xz-plane)		Azimuth plane (yz-plane)	
	Single patch	Array	Single patch	Array
Simulation	77°	16°	64°	66°
Measurement	76°	18°	57°	65°

array worn on the back, inside the jacket (Figure 2). The same array is used for the beamforming and space-time coding scenarios.

The transmission is performed in frames, transmitting at a rate of 1 Msymbols per second. Each transmitted frame is simultaneously used for both beamforming and space-time coding and consists of the following symbols.

(i) Binary (BPSK phase shift keyed) pilot symbols for each transmit antenna sent in separate time slots to avoid interference of pilot symbols from different transmit antennas at the receiver. These pilot symbols are exploited at the receiver for estimating symbol timing, carrier frequency offset, and complex channel gains.

(ii) Quadrature (QPSK phase shift keyed) data symbols encoded according to the 3/4 rate orthogonal space-time code documented in [27, pp 194 (5.143)].

(iii) Uncoded QPSK symbols, equal on all transmit channels but with phase increments at the antenna terminals in multiples of 15° to generate beams in the $-10°, \ldots, +10°$ elevation range.

A guard interval is inserted between consecutive frames. From the signals received during the guard intervals the, noise variance is estimated.

Transmitted beams can be steered with main beams oriented along small-elevation angles around broadside, without the generation of grating lobes in the radiation pattern. The elevation angle θ is zero when all array elements are driven in phase. Beams at other elevation angles are produced by driving the subsequent antenna patches of the array with a phase increment $\Delta\varphi = \varphi_2 - \varphi_1 = \varphi_3 - \varphi_2 = \varphi_4 - \varphi_3$, with φ_n denoting the phase rotation applied to the nth transmit antenna ($n = 1, 2, 3, 4$). The relation between the phase angle increment $\Delta\varphi$ and elevation angle θ is given by

$$\Delta\varphi = \frac{2\pi d}{\lambda}\sin(\theta) \approx \frac{2\pi d}{\lambda}\theta. \quad (1)$$

The approximation is valid for small-elevation angles and, with $d = 92$ mm and $\lambda = 122$ mm at 2.45 GHz, results in $\Delta\varphi \approx 4.74 \cdot \theta$. A phase increment of $\Delta\varphi = 15°$ at the antenna terminals, equal to the phase step size applied in the transmission, corresponds to an increment of $\theta \approx 3.2°$ in the main beam's elevation angle. The performance for a beam with a given elevation angle is assessed by

selecting the received symbols that have been transmitted with the corresponding phase increment on subsequent antenna patches.

The transmit power configured for each antenna is +0 dBm for the LoS and +20 dBm for the NLoS measurements in order to compensate for the average path loss experienced in the specific propagation conditions. The signals received in this way are always well above the receiver noise floor but always below the level that causes saturation of the receivers' analog-to-digital converters.

Denoting by $s_n^{(i)}(k)$ the kth signal sample transmitted by the nth antenna during the ith frame, in case of beamforming, we have $s_n^{(i)}(k) = a^{(i)}(k)e^{j\varphi_n}$, where $a^{(i)}(k)$ is a QPSK symbol with

$$E\left[\left|a^{(i)}(k)\right|^2\right] = \sigma_a^2. \tag{2}$$

The transmitted energy per information bit is denoted as $E_{b,\mathrm{tr}}$, the total (sum over all antennas) transmitted energy per symbol interval (for QPSK) is $4\sigma_a^2 = 2E_{b,\mathrm{tr}}$, so that $E_{b,\mathrm{tr}} = 2\sigma_a^2$. In case of space-time coding, we consider an orthogonal block code with the following codeword structure [27, pp 194 (5.143)]:

$$\mathbf{C} = \begin{bmatrix} a_1 & -a_2^* & -a_3^* & 0 \\ a_2 & a_1^* & 0 & -a_3^* \\ a_3 & 0 & a_1^* & a_2^* \\ 0 & a_3 & -a_2 & a_1 \end{bmatrix}. \tag{3}$$

The row and column indices refer to the transmit antenna and the time slot, respectively. The nonzero entries of $\mathbf{C}$ are QPSK symbols with variance σ_a^2. Denoting by $\mathbf{C}^{(i)}(l)$ the lth codeword transmitted during the ith frame, we have $s_n^{(i)}(4l + p) = (\mathbf{C}^{(i)}(l))_{n,p}$ for $p = 0, 1, 2, 3$. The total (sum over all antennas) transmitted energy per symbol interval is $3\sigma_a^2 = (1/4) \cdot 6E_{b,\mathrm{tr}}$, yielding $E_{b,\mathrm{tr}} = 2\sigma_a^2$.

For the space-time code, only three out of four antennas are transmitting in each time slot, reducing the total transmitted power by a factor 3/4 as compared to beamforming. However, since only three information symbols are transmitted in four time slots, the useful symbol rate is also reduced by a factor 3/4. Therefore, the total transmitted energy per information bit $E_{b,\mathrm{tr}}$ is the same for the space-time code and for the beam former.

3.2. Base Station: Receiving System. The receiving antenna array is displayed in Figure 3 and consists of four vertically polarized dipole antennas equally spaced at 32 cm (2.6λ) apart and with its phase center 1.25 m above the floor level. The antenna array is directly connected to a Signalion HaLo 430 MIMO transceiver unit, synchronously sampling the received signals after conversion to baseband. The obtained I and Q samples are stored on a hard disk for later processing.

Based on the stored I and Q samples, carrier frequency offset and timing correction are applied, and matched filter output samples (at the symbol rate) are computed. The

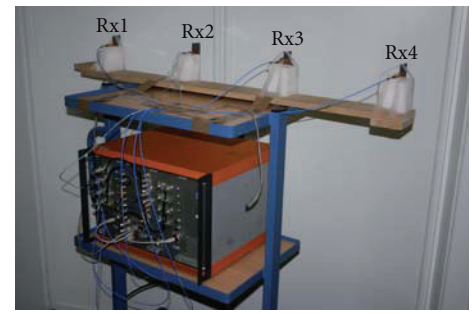

Figure 3: The fixed receiving antenna array with four vertical dipoles.

sample corresponding to the mth receive antenna during kth symbol interval in ith frame can be represented by

$$r_m^{(i)}(k) = \sum_{n=1}^{4} h_{m,n}^{(i)} s_n^{(i)}(k) + w_m^{(i)}(k), \tag{4}$$

where $h_{m,n}^{(i)}$ denotes the channel gain from the nth transmit antenna to the mth receive antenna, and $w_m^{(i)}(k)$ is a Gaussian noise contribution with

$$E\left[\left|w_m^{(i)}(k)\right|^2\right] = N_{0,m}. \tag{5}$$

In the case of beamforming, the detection of the symbol $a^{(i)}(k)$ is based on maximum-ratio combining (MRC) of the samples $r_m^{(i)}(k)$, $m = 1, \ldots, 4$. The resulting SNR at the input of the detector corresponding to the ith frame is given by

$$\mathrm{SNR}_{\mathrm{Beam}}^{(i)} = \sum_{m=1}^{4} \mathrm{SNR}_{\mathrm{Beam},m}^{(i)}, \tag{6}$$

where

$$\mathrm{SNR}_{\mathrm{Beam},m}^{(i)} = \frac{\sigma_a^2}{N_{0,m}} \left| \sum_{n=1}^{4} h_{m,n}^{(i)} e^{j\varphi_n} \right|^2 \tag{7}$$

is the ratio of signal power to noise power in $r_m^{(i)}(k)$.

In the case of space-time coding, the detection of an information symbol contained in the codeword $\mathbf{C}^{(i)}(l)$ is based on the MRC of the samples $r_m^{(i)}(4l + p)$, $m = 1, \ldots, 4$, $p = 0, \ldots, 3$. The resulting SNR at the input of the detector corresponding to the ith frame is given by

$$\mathrm{SNR}_{\mathrm{STC}}^{(i)} = \sum_{m=1}^{4} \mathrm{SNR}_{\mathrm{STC},m}^{(i)}, \tag{8}$$

where

$$\mathrm{SNR}_{\mathrm{STC},m}^{(i)} = \frac{\sigma_a^2}{N_{0,m}} \sum_{n=1}^{4} \left| h_{m,n}^{(i)} \right|^2 \tag{9}$$

is the ratio of signal power to noise power after the proper combining of $r_m^{(i)}(4l + p)$, $p = 0, \ldots, 3$.

In the following, we will consider the instantaneous E_b/N_0 ratio at the detector input, which in the case of QPSK is defined as SNR/2, where SNR equals $\mathrm{SNR}^{(i)}_{\mathrm{Beam}}$ or $\mathrm{SNR}^{(i)}_{\mathrm{STC}}$, depending on the transmit scenario. The average E_b/N_0 ratio is obtained by averaging the instantaneous E_b/N_0 over the frame index i. When no receiver diversity is exploited, only the signal from one receive antenna is processed; in this case, the summations in (6) and (8) contain only one term.

3.3. Measurement Scenario. The propagation environment for the measurements is an office environment at Ghent University, in a building from the 1930s with very solid brick walls.

Office equipment such as metal closets as well as the presence of people also have an important influence on the indoor radio propagation. A floor plan of the environment is displayed in Figure 4. The path between the markers A and B is an LoS path, whereas the sideways path labeled A to C is NLoS. In the latter case, the direct signal path is blocked by two solid brick walls. Measurements described in [2] confirm the Rayleigh-distributed small-scale fading experienced along this sideway's path.

4. Measurement Results and Analysis

The beamforming results documented in this section are calculated based on the symbols transmitted with a phase increment corresponding to a zero-elevation beam when the array is worn by the firefighter. The values $\mathrm{SNR}^{(i)}_{\mathrm{Beam},m}$ are obtained by measuring the SNR of the corresponding samples $r^{(i)}_m(k)$. According to (7), $\mathrm{SNR}^{(i)}_{\mathrm{Beam},m}$ could in principle be obtained from the measured channel gains $h^{(i)}_{m,n}$ and the phases φ_n applied to transmit antenna signals; however, this method gave rise to less accurate results, due to channel estimation errors and variations of the channel gains over a frame. For space-time coding, the samples $r^{(i)}_m(4l+p)$, $p = 0,\ldots,3$ are properly combined using the channel estimates derived from the pilot symbols, and the values $\mathrm{SNR}^{(i)}_{\mathrm{STC},m}$ are obtained by measuring the SNR of the samples that result from this combining. The signals on all four receive antennas are recorded synchronously. To assess the performance without receiver diversity, the signal of only one antenna was used (RX3 in Figure 3). When relying on receiver diversity, MRC is applied to the signals from all four antennas. The wearable antenna array, deployed on the rescue worker as documented in Section 2, is used for both the beamforming scenario and the space-time coding scenario, to allow a fair performance comparison.

4.1. Beamforming Calibration Measurement. The actual phase relationship of the signals at the transmit antenna array is influenced by the lengths of the transmission lines feeding the antenna patches. Hence, first a calibration measurement is performed using an RF combiner to join the signals at the ends of the transmission lines (to be connected to the antenna ports later). The combined signal is then connected to the receiver via a 60 dB attenuator. The phase relationships between the different transmit chains are then adjusted in order to achieve the maximum amplitude for a zero-phase increment.

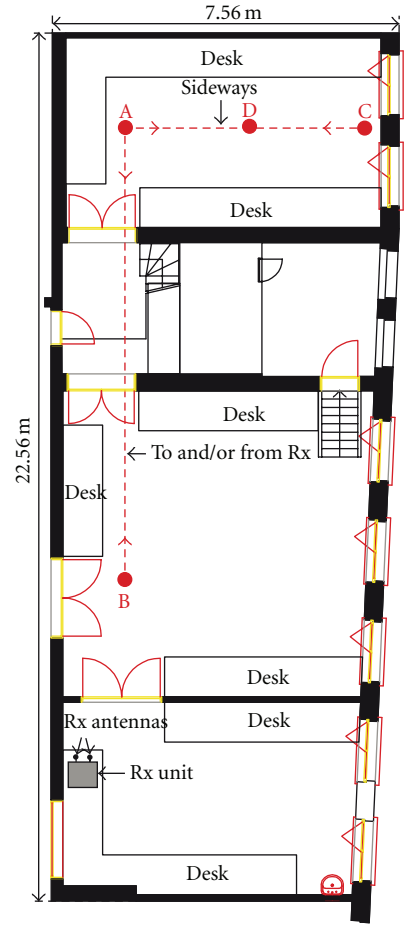

FIGURE 4: Floor plan of the indoor environment where the measurement campaign was performed.

Additionally, when the array is positioned on the human body, a tilt of a few degrees in the elevation plane is expected, for which compensation is desirable. Therefore, a second calibration measurement is performed with the firefighter standing straight and the array oriented towards the receiver, at 10 m distance.

For various beam elevation angles, Figure 5 shows the average of $\mathrm{SNR}^{(i)}_{\mathrm{Beam}}$ over all frames after calibration, normalized to 0 dB for the 0° elevation beam. The beam elevation range is limited to $-10°,\ldots,+10°$ to avoid grating lobes in the radiation pattern. The three curves correspond to the following propagation conditions.

4.1.1. Non-Line-of-Sight. In NLoS conditions, the signals are propagated by means of multiple scattered reflections in the environment. Here, beamforming is clearly not advantageous anymore. In our measurement, the higher elevation angles provided somewhat stronger signals, possibly because of propagation over the top of metal closets in the office.

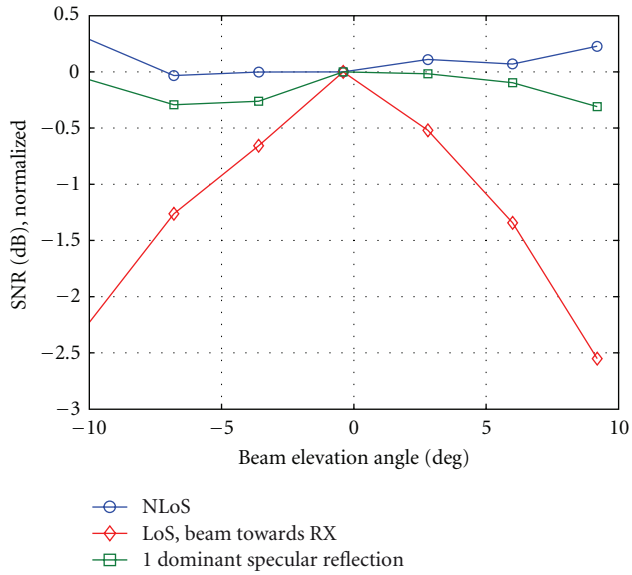

FIGURE 5: Average SNR as a function of the beam elevation angle, in the LoS environment, with the main beam directed towards and away from the receiver, as well as in the NLoS environment. The SNR is normalized to 0 dB for the 0° elevation beam.

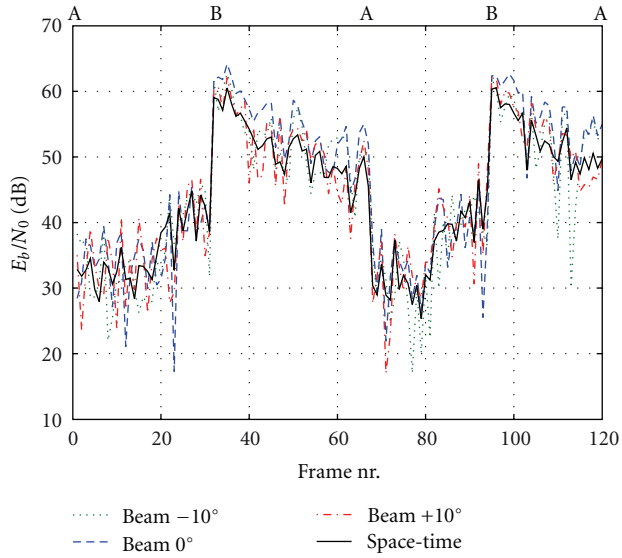

FIGURE 6: E_b/N_0 along the line-of-sight path, without receiver diversity (no MRC) for −10°, 0°, and +10° beams and for the space-time code. Labels on top indicate locations on the floor plan.

4.1.2. LoS, Beam towards the Receiver. The measured SNR demonstrates the correct implementation of the beamforming. The zero-elevation beam clearly provides the highest SNR. Note that the values in Table 2 are for anechoic conditions, whereas the LoS curve in Figure 5 is measured in the actual indoor environment. The measured beamwidth is larger, probably due to ground and ceiling reflections.

4.1.3. A Single Dominant Specular Reflection. With the beam oriented away from the receiver, the propagation is assumed to predominantly occur via a single reflection in the indoor environment. The difference in SNR for different beam angles is smaller but the zero-elevation beam still provides the strongest signal.

4.2. Line-of-Sight Path. For the measurements along the LoS path, the rescue worker walks between the points marked A and B in the floor plan, Figure 4. The plots in Figures 6 and 7, displaying the E_b/N_0 per frame for the LoS scenario, correspond to the walk sequence ABABA. Clearly, shadowing effects by the human body cause an additional attenuation of the signal when the antenna array is oriented away from the receiver. Note that, as the antenna array is worn on the back, the beam is oriented away from the receiver when the test person approaches the base station (from A to B). A steep change in E_b/N_0, by more than 15 dB, is noticed each time the rescue worker turns around, reorienting the beam.

4.2.1. Reception without Receiver Diversity. Without receiver diversity, the E_b/N_0 recorded for the beamforming results from a constructive addition of the received electromagnetic fields generated by each transmit antenna n (see (7)). For the space-time code, the E_b/N_0 results from the addition of the powers received from each transmit antenna n (see (9)). The results for reception in LoS conditions without receiver diversity are displayed in Figure 6.

(i) Line-of-sight (beam towards RX).

(a) The beamforming achieves E_b/N_0 values that are a few dB larger compared to using the space-time code. If the receive antennas were located at zero-elevation angle and assuming identical additive white Gaussian noise (AWGN) channels between the transmit and receive antennas, the difference in E_b/N_0 between beamforming and space-time coding would amount to 6 dB, which corresponds to the difference between the constructive addition of the received electromagnetic fields at the receive antenna elements along the main beam direction of the array (beamforming) and the addition of the powers in case of transmit diversity (by means of space-time coding).

(b) The zero-elevation beam concentrates the transmitted power towards the receiver. The azimuth angle is much wider (Table 2), allowing considerable rotation of the body in the azimuth plane while maintaining a good communication link.

(ii) A single dominant specular reflection (beam away from RX).

(a) The beam and the space-time code approximately exhibit equal performance, when considering average E_b/N_0 over all received frames.

The measured behavior, with the zero-elevation beam providing the strongest signal compared to beams with other elevations, indicates the presence of low-elevation reflections of the transmitted beam on vertical surfaces such as walls and metal closets.

(b) The variance of the signal level is larger for the beamforming case, known to cause a worse BER for the same average E_b/N_0. No transmit diversity is present in the beamforming case whereas fourth-order transmit diversity is achieved by the space-time code. In Figure 6, less signal fading occurs for the space-time coded transmission, especially with the beam oriented away from the receiver.

4.2.2. Reception with Fourth-Order Receiver Diversity. The results for reception in LoS conditions with fourth-order receiver diversity are displayed in Figure 7.

(i) Line-of-sight (beam towards RX).

(a) The E_b/N_0 values for the zero-elevation beam are now often 6 dB higher than for the space-time code.

(b) Thanks to the receiver diversity, the transmission relying on beamforming suffers less degradation due to fading. The signal dips in Figure 7 are less deep than in Figure 6.

(ii) A single dominant specular reflection (beam away from RX).

(a) Even with the beam oriented away from the receiver, zero-elevation beamforming still performs better (in terms of average E_b/N_0) than space-time coding, since the propagation in LoS conditions predominantly occurs by means of a small number of low-elevation angle reflections at walls and office equipment.

(b) The beam transmission corresponds to a 1×4 MIMO link and the space-time code to a 4×4 MIMO system. Therefore, less signal fading occurs for the space-time coded transmission, especially with the beam oriented away from the receiver.

4.3. Non-Line-of-Sight. For the NLoS measurements, the rescue worker walks back and forth between the points marked A and C in the floor plan, Figure 4. The measurement results are displayed in Figures 8 and 9. As the propagation link is composed of a sum over an ensemble of nondominant multipaths created by reflection/transmission/diffraction, the E_b/N_0 varies dramatically for subsequent frames. Note that 20 dB extra transmit power is used to compensate for the associated signal attenuation.

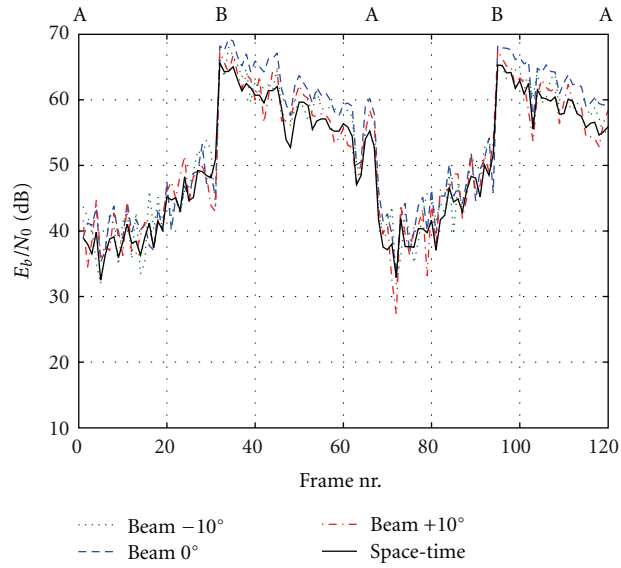

FIGURE 7: E_b/N_0 along the line-of-sight path, with receiver diversity (MRC) for −10°, 0°, and +10° beams and for the space-time code. Labels on top indicate locations on the floor plan.

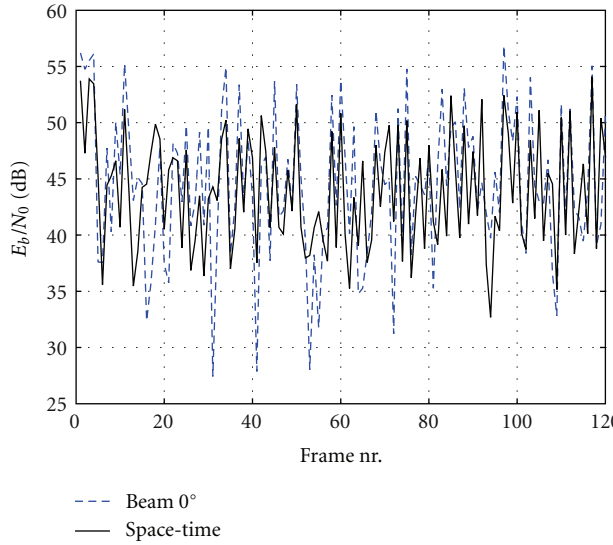

FIGURE 8: E_b/N_0 in non-line-of-sight conditions, without receiver diversity (no MRC). NLoS transmissions performed at 20 dB extra power compared to LoS transmissions.

4.3.1. No Receiver Diversity. The results for beamforming in NLoS conditions without receiver diversity are displayed in Figure 8. Without receiver diversity the beamforming performs clearly worse than the space-time code. Deep fades occur due to the lack of transmit diversity, gain for the static beamforming case. The space-time code realizes fourth-order transmit diversity, decreasing the fluctuation in E_b/N_0.

4.3.2. Fourth-Order Receiver Diversity. The results for beamforming in NLoS conditions with fourth-order receiver diversity are displayed in Figure 9. With receiver diversity, the

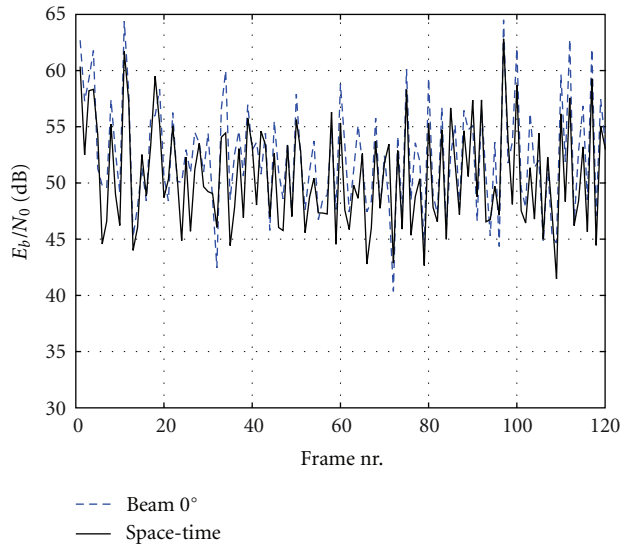

FIGURE 9: : E_b/N_0 in non-line-of-sight conditions, with receiver diversity (MRC). NLoS transmissions performed at 20 dB extra power compared to LoS transmissions.

variation of E_b/N_0 caused by fading is reduced, also for the beamforming case.

4.4. Minimum, Average, and Maximum E_b/N_0. The minimum, average, and maximum E_b/N_0 values recorded for each measurement are listed in Table 3. The beamforming always achieves higher average received E_b/N_0 values (the associated power gain is listed in the last column of Table 3), indicating the important contribution of signals reflected or scattered at low-elevation angles in the indoor propagation environment. Simulation results in [5] also indicated that beamforming maximizes the received SNR.

The minimum E_b/N_0 values are generally higher for the space-time code especially in absence of receive diversity gain. Lower minimum E_b/N_0 values indicate more severe fading, resulting in a higher BER for a given average E_b/N_0 value. Higher maximum E_b/N_0 values always result for the beamforming case, caused by concentrating the transmitted power in a range of low-elevation angles. However, the average BER is mostly determined by the lowest E_b/N_0 values occurring.

The results indicate that some degree of diversity is always beneficial, even in LoS conditions. MRC of 4 signals, received on separate antennas, provides array gain and additional diversity gain. The average measured total additional gain by receiving on 4 antennas using MRC varies between 5.9 and 6.8 dB for all measured cases in Table 3.

4.5. BER Characteristics. For QPSK, the BER for the ith frame is given by

$$\mathrm{BER}^{(i)} = Q\left(\sqrt{\left(\frac{2E_b}{N_0}\right)^{(i)}}\right), \tag{10}$$

where $Q(x)$ is the tail area (from x to ∞) of the zero-mean univariate Gaussian distribution, and $(E_b/N_0)^{(i)}$ is the E_b/N_0 value at the input of the detector corresponding to the ith frame, which equals $(1/2)\cdot \mathrm{SNR}^{(i)}_{\mathrm{Beam}}$ or $(1/2)\cdot \mathrm{SNR}^{(i)}_{\mathrm{STC}}$ depending on the transmit scenario. The displayed BER is the average of $\mathrm{BER}^{(i)}$ over the frame index i. The detailed procedure for calculating measurement-based BER characteristics for a range of average E_b/N_0 values is outlined in [2]. In case of fourth-order receiver diversity, we obtain receive array gain (which equals 6 dB in case of identical powers on each receive antenna), with an additional diversity gain. The bit error rate represented allows a performance comparison of our experimental transmissions for beamforming and space-time coding with or without receiver diversity. Note that beamforming and space-time coding transmissions are performed within the same transmission frame, hence with equal momentary propagation conditions.

To obtain a fair comparison of the BER produced by beamforming versus space-time coding, we consider an equal total transmitted energy per information bit $E_{b,\mathrm{tr}}$ for both scenarios. Therefore, we introduce the notion of normalized average E_b/N_0, which equals either the average E_b/N_0 at the detector output (in the case of STC) or the average E_b/N_0 at the detector output minus the beamforming power gain from Table 3 (in the case of beamforming). This way displaying BER curves as a function of the normalized E_b/N_0 includes the power gain associated with coherent beamforming.

4.5.1. Non-Line-of-Sight. Figure 10 lists the BER characteristics for the measurements along the NLoS path. Due to the absence of diversity, the curve in case of beamforming, as received on RX3, approaches the theoretical curve for Rayleigh fading. Without receiver diversity, relying only on RX3, at higher E_b/N_0 the BER decreases more quickly for links relying on the space-time code than for the beamforming link thanks to the inherent transmit diversity of the former. For the beamforming, there is no diversity at all in this case, hence we are comparing fourth and first order diversity systems. Space-time coding performs better than beamforming when the BER $< 8.6\cdot 10^{-2}$.

With receiver diversity, the curves for the space-time code also decrease faster than for the beamforming case, thanks to the higher diversity order. However, the difference is not so large for low-to-moderate E_b/N_0 values, as we are now comparing a 4×4 MIMO link with a 1×4 SIMO system. They exhibit 16th- and fourth-order diversity, respectively, and the additional performance gain associated to increasing the diversity order from 4 to 16 is not that large anymore. The space-time code performs better than beamforming when the BER $< 3.3\cdot 10^{-3}$. To achieve a BER $= 10^{-4}$, the space-time code requires 1.4 dB less transmit energy per information bit. Measurements documented in [7], although focused on channel capacity, also indicated the better performance of space-time coding at higher SNR levels. Note that beamforming is also more sensitive to movements of the rescue worker, as bending of the body will point the beam upward or downward.

Table 3: E_b/N_0 for STC and beamforming; beamforming power gain.

	STC (dB)	Beamforming (dB)	Beamforming power gain (dB)
NLoS, no receive diversity			
min.	29.7	25.9	
avg.	43.7	45.5	1.8
max.	51.1	53.8	
NLoS, fourth-order receive diversity			
min.	38.4	36.5	
avg.	50.2	52.2	2.0
max.	59.8	62.5	
LoS, no receive diversity			
min.	43.1	38.6	
avg.	49.9	53.3	3.4
max.	57.5	60.5	
LoS, fourth-order receive diversity			
min.	49.7	51.9	
avg.	56.6	60.1	3.5
max.	62.0	65.5	
A single dominant specular reflection, no receive diversity			
min.	22.3	13.1	
avg.	33.4	34.9	1.5
max.	40.2	42.9	
A single dominant specular reflection, fourth-order receive diversity			
min.	29.5	29.7	
avg.	39.3	41.0	1.7
max.	45.3	49.0	

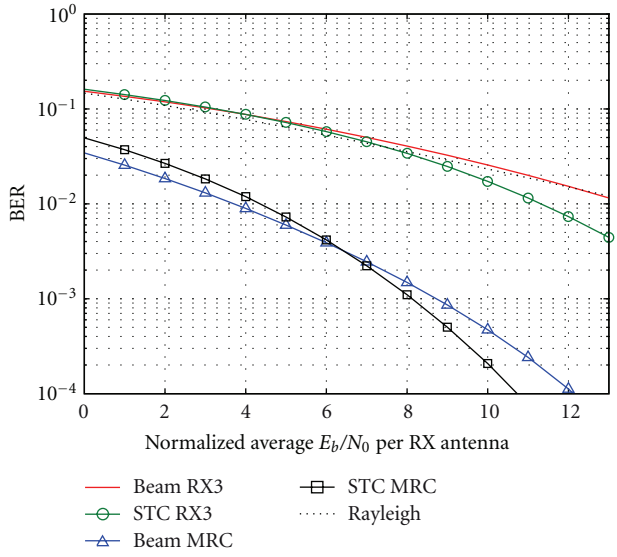

Figure 10: BER as a function of the normalized average E_b/N_0 per receive antenna, recorded along the NLoS path, for transmissions at equal total $E_{b,\mathrm{tr}}$.

4.5.2. Line-of-Sight. The BER characteristics for the LoS path are calculated separately for the frames where the beam is oriented towards the receiver and those with the beam directed away from it. Figure 11 displays the BER characteristics for the frames recorded in LoS, with the beam oriented towards the receiver. The curve for beamforming without diversity is now better than the theoretical curve for Rayleigh fading. The signal propagation, composed of a strong LoS component and some reflected signals, produces a large power gain for the transmission relying on beamforming. BER curves for the set of frames measured with the beam oriented towards the receiver display a considerable performance improvement in case of transmit beamforming with receiver diversity. Concentrating the transmitted power along the low-elevation angles creates a significantly stronger signal at the receiver. To achieve a BER $= 10^{-4}$, the beamforming requires 2.3 dB less transmit energy per information bit.

4.5.3. A Single Dominant Specular Reflection. The BER curves in Figure 12 correspond to the set of frames measured along the LoS path, with the beam oriented away from the receiver. The characteristic for beamforming without diversity approaches the theoretical Rayleigh fading characteristic, indicating the blockage of the direct signal path by the human body. Additionally, the antenna array's main beam is now directed away from the receiver. The performance of beamforming with receiver diversity is always slightly

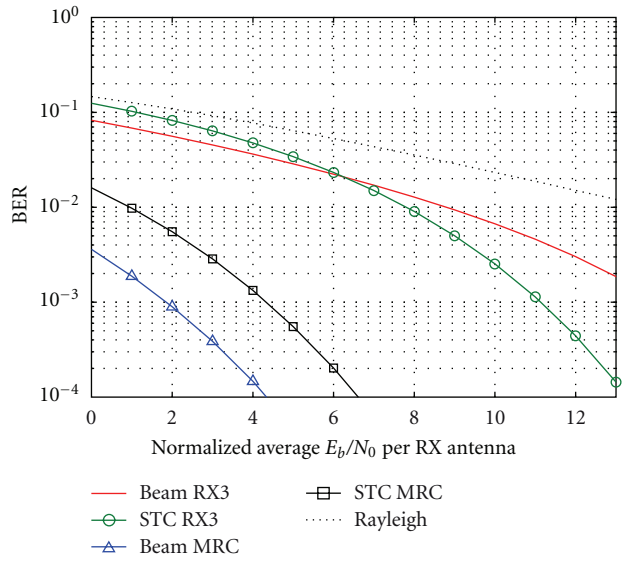

Figure 11: BER as a function of the normalized received E_b/N_0 per antenna, recorded along the LoS path with the transmit antenna array oriented towards the receiver, for transmissions at equal total $E_{b,\mathrm{tr}}$.

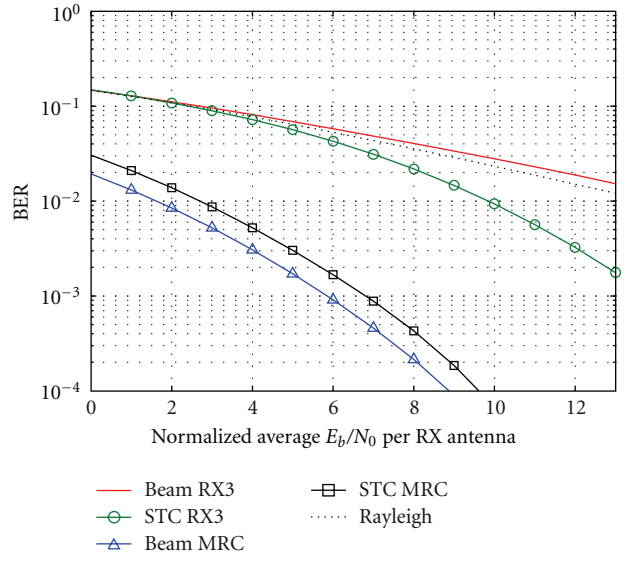

Figure 12: BER as a function of the normalized received E_b/N_0 per antenna, for communication via a single dominant specular reflection and transmissions at equal total $E_{b,\mathrm{tr}}$.

better than for space-time coding. The propagation is mainly realized through one dominant specular reflection, occuring at a low-elevation angle. To achieve a BER $= 10^{-4}$, the beamforming requires 0.7 dB less transmit energy per information bit, with the beam oriented away from the receiver.

Table 4: Signal envelope correlation of the received signals.

	RX1	RX2	RX3	RX4
NLoS, zero-elevation beam				
RX1	1	0.49966	0.46488	0.37184
RX2	0.49966	1	0.49911	0.51818
RX3	0.46488	0.49911	1	0.58911
RX4	0.37184	0.51818	0.58911	1
LoS, zero-elevation beam				
RX1	1	0.64439	0.64289	0.64433
RX2	0.64439	1	0.53591	0.54072
RX3	0.64289	0.53591	1	0.55964
RX4	0.64433	0.54072	0.55964	1
A dominant specular reflection, zero-elevation beam				
RX1	1	0.55218	0.43311	0.19448
RX2	0.55218	1	0.58084	0.42663
RX3	0.43311	0.58084	1	0.58893
RX4	0.19448	0.42663	0.58893	1

4.6. Signal Envelope Correlation. The normalized correlation coefficients of the signal envelopes are given by

$$\rho_{X,Y} = \frac{E[X \cdot Y] - E[X]E[Y]}{\sqrt{\left[E[X^2] - (E[X])^2\right]\left[E[Y^2] - (E[Y])^2\right]}}. \quad (11)$$

For the transmit correlation, as seen from antenna RX3, we set $X = |h_{3,n_1}|$ and $Y = |h_{3,n_2}|$, with n_1 and n_2 the indices of the corresponding TX antennas. The used channel estimation values $h_{i,j}$ are based on the received pilot symbols. For the receive correlation, X and Y are the magnitudes of the zero-elevation beam symbols as received on the corresponding RX antennas.

4.6.1. Correlation Coefficients of the Received Signals. Table 4 lists the correlation coefficients for the received signals, for reception of the zero-elevation beam. A significant diversity gain may be realized when the envelope correlation coefficient is lower than 0.7 [28], which is the case for all receive correlation values. MRC reception with multiple antennas will produce array and diversity gain in all cases. An interesting observation is the decreasing correlation for receive antennas spaced further apart in the NLoS and specular reflection cases (Figure 3 shows the RX antenna positions). For the LoS case, as expected for a beam directed towards the receiver along a LoS path, the correlation is higher and more constant as a function of RX antenna separation.

4.6.2. Correlation Coefficients of the Transmitted Signals. Table 5 displays the correlation coefficients for the signals transmitted by different patches of the off-body array. The values are rather high for all cases, due to the proximity of the human body. Remarkably, the correlation is the lowest for the upper two patches (TX1 and TX2) in the array. This value is below 0.7 for all cases and allows a significant transmit

Table 5: Signal envelope correlation of the transmitted signals

	TX1	TX2	TX3	TX4
NLoS, as received by RX3				
TX1	1	0.60868	0.73301	0.76079
TX2	0.60868	1	0.84735	0.86725
TX3	0.73301	0.84735	1	0.99728
TX4	0.76079	0.86725	0.99728	1
LoS, as received by RX3				
TX1	1	0.66085	0.67815	0.72005
TX2	0.66085	1	0.85092	0.87672
TX3	0.67815	0.85092	1	0.99662
TX4	0.72005	0.87672	0.99662	1
A dominant specular reflection, as received by RX3				
TX1	1	0.56683	0.74630	0.76840
TX2	0.56683	1	0.83224	0.84849
TX3	0.74630	0.83224	1	0.99781
TX4	0.76840	0.84849	0.99781	1

diversity gain [28] for the space-time code. The other signals will also provide some diversity but in a minor way. The correlation is very high for the lower two patches (TX3 and TX4). As the array is perfectly symmetrical, we assume that this is an effect of the proximity to the floor.

5. Conclusions

Experimentally comparing static beamforming and transmit diversity techniques based on space-time codes for a wearable vertical textile, antenna array consisting of four radiating patches worn on the back of a firefighter walking in an indoor environment leads to the following conclusions.

While the measured average E_b/N_0 values at the input of the detector are always higher for the beamforming system, the variation of the signal level is more severe due to the limited diversity, resulting in worse bit error characteristics.

Without receiver diversity, the bit error rate curves indicate that, for any bit error rate of practical use (BER $< 2.1 \cdot 10^{-2}$), space-time coding performs best for line-of-sight as well as for non-line-of-sight conditions. In the indoor environment, some degree of diversity, is desired to combat the severe fading that is present on the signals.

With fourth-order receiver diversity in line-of-sight conditions, beamforming always performs better than space-time coding. The presence of both transmit beamforming and receive diversity results in a higher average received E_b/N_0 while the effects of fading are also reduced. In non-line-of-sight conditions, however, space-time coding is better as soon as BER $< 3.3 \cdot 10^{-3}$. The relative advantage of space-time coding for higher SNR levels was also observed in [7].

An important aspect to take into account is that the beamforming system is more sensitive to body movements, such as bending over, changing the elevation angle of the main beam. Switching to space-time coding results in a larger beam width in the elevation plane.

Static beamforming, however, can be realized by using phase shifters, whereas space-time coding requires expensive and more power-consuming hardware with dedicated transmit chains for each channel.

Further research will involve an extension of the system presented in this contribution, deploying two textile antenna arrays, worn at the front and the back of the human body, realizing a significant additional improvement by countering the effect of shadowing by the human body. Also, a hybrid system that combines static beamforming and space-time coding will be studied experimentally.

Acknowledgment

This work was supported by the fund for Scientific Research-Flanders (FWO-V) by project "Advanced space-time processing techniques for communication through multi-antenna systems in realistic mobile channels."

References

[1] D. Curone, E. L. Secco, A. Tognetti et al., "Smart garments for emergency operators: the ProeTEX project," *IEEE Transactions on Information Technology in Biomedicine*, vol. 14, no. 3, pp. 694–701, 2010.

[2] P. Van Torre, L. Vallozzi, C. Hertleer, H. Rogier, M. Moeneclaey, and J. Verhaevert, "Dynamic link performance analysis of a rescue worker's off-body communication system using integrated textile antennas," *IET Science, Measurement and Technology*, vol. 4, no. 2, pp. 41–52, 2010.

[3] S. Cotton and W. Scanlon, "An experimental investigation into the influence of user state and environment on fading characteristics in wireless body area networks at 2.45 GHz," *IEEE Transactions on Wireless Communications*, vol. 8, no. 1, Article ID 4786471, pp. 6–12, 2009.

[4] L. Vallozzi, P. Van Torre, C. Hertleer, H. Rogier, M. Moeneclaey, and J. Verhaevert, "Wireless communication for firefighters using dual-polarized textile antennas integrated in their garment," *IEEE Transactions on Antennas and Propagation*, vol. 58, no. 4, Article ID 5398858, pp. 1357–1368, 2010.

[5] C. van Rensburg and B. Friedlander, "Transmit diversity for arrays in correlated Rayleigh fading," *IEEE Transactions on Vehicular Technology*, vol. 53, no. 6, pp. 1726–1734, 2004.

[6] L. Chu, J. Yuan, and Z. Chen, "A coded beamforming scheme for frequency-flat MIMO fading channels," *IET Communications*, vol. 1, no. 5, pp. 1075–1081, 2007.

[7] C. Hermosilla, R. A. Valenzuela, L. Ahumada, and R. Feick, "Empirical comparison of MIMO and beamforming schemes for outdoor-indoor scenarios," *IEEE Transactions on Wireless Communications*, vol. 8, no. 3, Article ID 4801460, pp. 1139–1143, 2009.

[8] C. Hermosilla, R. Feick, R. Valenzuela, and L. Ahumada, "Improving MIMO capacity with directive antennas for outdoor-indoor scenarios," *IEEE Transactions on Wireless Communications*, vol. 8, no. 5, Article ID 4927423, pp. 2177–2181, 2009.

[9] X. Chen, Y. Gong, and Y. Gong, "Suppression of directional interference for STBC MIMO system based on beamforming," in *Proceedings of the International Conference on Communications, Circuits and Systems, (ICCCAS'06)*, pp. 983–987, June 2006.

[10] L. Min, Y. Luxi, and Y. Xiaohu, "Adaptive transmit beamforming with space-time block coding for correlated MIMO fading channels," in *Proceedings of the IEEE International Conference on Communications, (ICC'07)*, pp. 5879–5884, June 2007.

[11] L. Ping, L. Zhang, and H. So, "On a hybrid beamforming/space-time coding scheme," *IEEE Communications Letters*, vol. 8, no. 1, pp. 15–17, 2004.

[12] G. Jongren, M. Skoglund, and B. Ottersten, "Combining beamforming and orthogonal space-time block coding," *IEEE Transactions on Information Theory*, vol. 48, no. 3, pp. 611–627, 2002.

[13] C. Sun and N. Karmakar, "Environment-oriented beamforming for space-time block coded multiuser MIMO communications," in *Proceedings of the Antennas and Propagation Society International Symposium*, pp. 1744–1747, IEEE, June 2004.

[14] K. Lin, Z. Hussain, and R. Harris, "Adaptive transmit eigenbeamforming with orthogonal space-time block coding in correlated space-time channels," in *Proceedings of the IEEE International Conference on Acoustics, Speech, and Signal Processing*, pp. V-817–V-820, May 2004.

[15] X. Cai and G. B. Giannakis, "Differential space-time modulation with eigen-beamforming for correlated MIMO fading channels," *IEEE Transactions on Signal Processing*, vol. 54, no. 4, pp. 1279–1288, 2006.

[16] L. Liu and H. Jafarkhani, "Application of quasi-orthogonal space-time block codes in beamforming," *IEEE Transactions on Signal Processing*, vol. 53, no. 1, pp. 54–63, 2005.

[17] H. Kim and J. Chun, "MIMO structure which combines the spatial multiplexing and beamforming," in *Proceedings of the 59th IEEE Vehicular Technology Conference, (VTC'04)*, pp. 108–112, May 2004.

[18] C. Lin, V. Raghavan, and V. Veeravalli, "To code or not to code across time: space-time coding with feedback," *IEEE Journal on Selected Areas in Communications*, vol. 26, no. 8, Article ID 4641968, pp. 1588–1598, 2008.

[19] Y. G. Kim and N. Beaulieu, "On MIMO beamforming systems using quantized feedback," *IEEE Transactions on Communications*, vol. 58, no. 3, Article ID 5426515, pp. 820–827, 2010.

[20] Y. Ko, Q. Ma, and C. Tepedelenlioğlu, "Comparison of adaptive beamforming and orthogonal STBC with outdated feedback," *IEEE Transactions on Wireless Communications*, vol. 6, no. 1, pp. 20–25, 2007.

[21] M. Kobayashi, G. Caire, and D. Gesbert, "Transmit diversity versus opportunistic beamforming in data packet mobile downlink transmission," *IEEE Transactions on Communications*, vol. 55, no. 1, pp. 151–157, 2007.

[22] S. Ekbatani and H. Jafarkhani, "Combining beamforming and space-time coding using noisy quantized feedback," *IEEE Transactions on Communications*, vol. 57, no. 5, pp. 1280–1286, 2009.

[23] S. S. Karimabadi, Y. Mohsenzadeh, A. R. Attari, and S. M. Moghadasi, "Bandwidth enhancement of single-feed circularly polarized equilateral triangular microstrip antenna," in *Proceedings of the Progress in Electromagnetic Research Symposium*, pp. 147–150, Hangzhou, China, March 2008.

[24] C. L. Tang, J. H. Lu, and K. L. Wong, "Circularly polarised equilateral-triangular microstrip antenna with truncated tip," *Electronics Letters*, vol. 34, no. 13, pp. 1277–1278, 1998.

[25] Y. S. Jawad and G. Debatosh, "Applications of triangular microstrip patch: circuit elements to modern wireless antennas," *Mikrotalasna Revija*, vol. 13, no. 1, pp. 8–11, 2007.

[26] Lion International (LDH group), 2011, http://lion-frankreich.lhd-gruppe.de/company.html.

[27] C. Oestges and B. Clerckx, *MIMO Wireless Communications: From Real-World Propagation to Space-Time Code Design*, Academic Press, 2007.

[28] S. M. Alamouti, "A simple transmit diversity technique for wireless communications," *IEEE Journal on Selected Areas in Communications*, vol. 16, no. 8, pp. 1451–1458, 1998.